

## Supporting Information

Morphology Transition in the Helical Tubules of Supramolecular Gel Driven by Metal Ions  
*Krishnamoorthy Lalitha,<sup>a</sup> Vellaisamy Sridharan,<sup>a</sup> C Uma Maheswari<sup>a</sup> Praveen Kumar Vemula,<sup>b</sup> and Subbiah Nagarajan<sup>a\*</sup>*

<sup>a</sup> Organic Synthesis Group, Department of Chemistry & The Centre for Nanotechnology and Advanced Biomaterials, School of Chemical and Biotechnology, SASTRA University, Thanjavur - 613401, Tamil Nadu, INDIA. Fax: 04362264120; Tel: 04362304270; E-mail: nagarajan@scbt.sastra.edu.

<sup>b</sup> Laboratory of Self-Assembled Biomaterials, Institute for Stem Cell Biology and Regenerative Medicine (inStem), National Centre for Biological Sciences (NCBS), Bangalore-560 065 India

### Table of Contents

1. Experimental Section	2
2. Synthesis	2
3. Gelation Studies	5
4. <b>Table S1.</b> Solvents/Oils used for gelation studies	5
5. <b>Figure S1.</b> (a-d) Photographs of gel formed by (a) <b>3b</b> in 1,2-DCB; (b) <b>3b</b> in olive oil; (c) <b>3c</b> in olive oil and (d) <b>3c</b> in 1,2-DCB.	7
6. <b>Figure S2.</b> Optical micrographs of (a) <b>3b</b> 1,2-DCB and (b) <b>3c</b> in 1,2-DCB. HRTEM images of (c & d) <b>3c</b> in 1,2-DCB, (e) <b>3b</b> in water and (f) <b>3c</b> in water.	7
7. <b>Figure S3.</b> ATR-FTIR spectra of GAP in powder form and helical tubular form.	7
8. <b>Figure S4.</b> Energy minimized structure of compound GAP.	8
9. <b>Figure S5.</b> HRTEM images of individual helical tubules in gel formed by GAP in 1,2-DCB displaying helical marking.	8
10. <b>Figure S6.</b> Mechanism for the formation of individual helical tubules in gel formed by GAP in 1,2-DCB displaying helical marking.	8
11. <b>Figure S7.</b> Response of gel formed by GAP in 1,2-DCB after the addition of Cu(OAc) <sub>2</sub> dissolved in water (a), Cu(OAc) <sub>2</sub> dissolved in ethanol:1,2-DCB (1:9 ratio) (b) and double distilled water (c).	9
12. <b>Figure S8.</b> HRTEM images of Cu <sup>2+</sup> induced randomly twisted fibers from helical tubules.	9
13. <b>Figure S9.</b> HRTEM image of fiber formation of GAP in water.	9
14. <b>Figure S10.</b> UV absorption spectra of gelator <b>3c</b> in 1,2-DCB.	10
15. <b>Figure S11.</b> (a-g) XPS spectra of helical tubules and randomly twisted fiber formation triggered by Cu <sup>2+</sup> fitted using Gaussian-Lorentzian peak	10
16. <b>Figure S12.</b> (a-e) Emission spectra of helical tubules in 1,2-DCB and its response to metal ions	11
17. <b>Figure S13.</b> Phase transition of gel formed by GAP in DCB in response to (a) Cu <sup>2+</sup> ; (b) Zn <sup>2+</sup> ; (c) Ca <sup>2+</sup> (d) Mg <sup>2+</sup> and (e) Al <sup>3+</sup> .	11
18. <b>Figure S14.</b> HRTEM images of GAP in 1,2-DCB in response to (a) Cu <sup>2+</sup> ; (b) Zn <sup>2+</sup> ; (c) Ca <sup>2+</sup> (d) Mg <sup>2+</sup> and (e) Al <sup>3+</sup> .	12
19. <b>Figure S15.</b> (a - d) Time course change of storage (G') and loss (G'') modulus	12
20. <b>Table S2.</b> Metal ion induced phase and morphological transition of gel formed by GAP in 1,2-DCB.	13

## Experimental Section

### Materials and General Methods

All reagents and solvents required for the synthesis were purchased from Sigma Aldrich, Merck, Alfa Aesar and, Avra chemicals, and were used as such without further purification. LR grade solvents were used to purify the compounds and distilled solvents were used, when necessary. The reaction progress was monitored by thin-layer chromatography using pre-coated silica gel plates purchased from Merck and visualized by UV detection or molecular iodine.

### Characterization Methods

$^1\text{H}$ - and  $^{13}\text{C}$ - NMR spectra were recorded on a Bruker Avance 300 MHz instrument in  $\text{DMSO-}d_6$  at room temperature. Chemical shifts ( $\delta$ ) are reported in parts per million (ppm) with respect to internal standard TMS and coupling constants ( $J$ ) are given in Hz. Proton multiplicity is assigned using the following abbreviations: singlet (s), doublet (d), triplet (t), quartet (q), multiplet (m). Electrospray ionization mass spectra (ESI-MS) were carried out in positive mode with a Thermo Fisher LCQ Advantage Max. Instrument by dissolving the solid sample in methanol. FT-IR spectra of GAP in powder and helical tube form were recorded as xerogel in an attenuated total reflectance (ATR) mode using PerkinElmer 100 FTIR Spectrometer in the spectral range of  $4000\text{ cm}^{-1}$  to  $500\text{ cm}^{-1}$ .

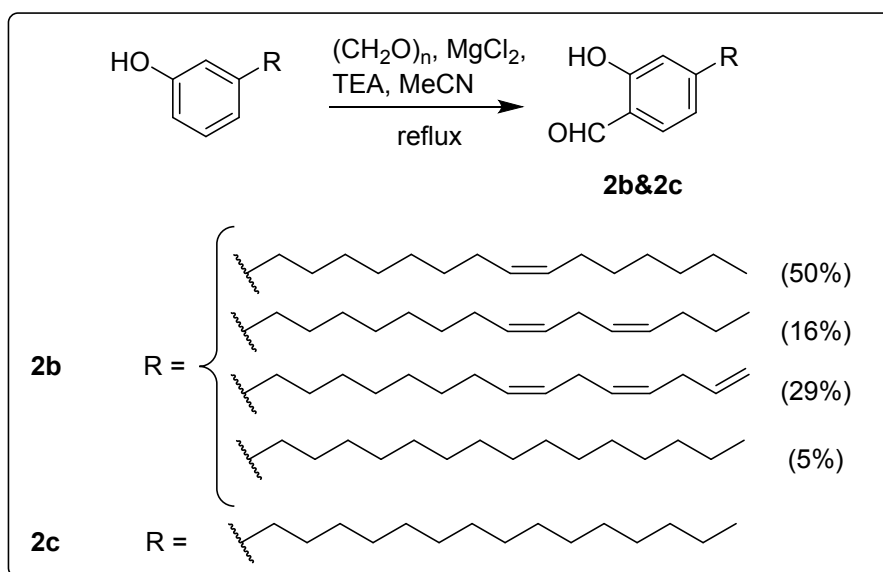
### Purification of Cardanol

The major constituent present in cashew nut shell liquid (CNSL) is cardanol, precursor of compounds 2b and 2c, a bio-based non isoprene lipid, comprising of phenolic lipid mixture: 5% of 3-*n*-pentadecylphenol (3-PDP), 50% of 3-(8Z-pentadecenyl) phenol, 16% of 3-(8Z, 11Z-pentadecadienyl) phenol and 29% of 3-(8Z,11Z,14-pentadecatrienyl) phenol. CNSL was distilled at a temperature between 210 and 280 °C, under a pressure from 2 to 8 mm Hg to get cardanol. Cardanol was obtained as pale yellow liquid which darkens during storage. After a second distillation, mixture of cardanol mono-, di- and tri-ene was obtained.

### Synthesis

#### General procedure for the synthesis of 2-hydroxy-4-alkylbenzaldehyde (2b and 2c)<sup>i</sup>

To a mixture of 3-alkyl phenol, (4 mmol), anhydrous magnesium chloride (6 mmol) and triethylamine (15 mmol) in acetonitrile (25 mL), dry paraformaldehyde (35 mmol) was added and heated under reflux for about 12-15 h. After the completion of the reaction as monitored by TLC, the reaction mixture was cooled to room temperature and 5% aq. HCl was added. The crude product was extracted with ethyl acetate, dried under  $\text{Na}_2\text{SO}_4$  and pure product was isolated by column chromatography using 95:5 v/v hexane-ethyl acetate as eluent

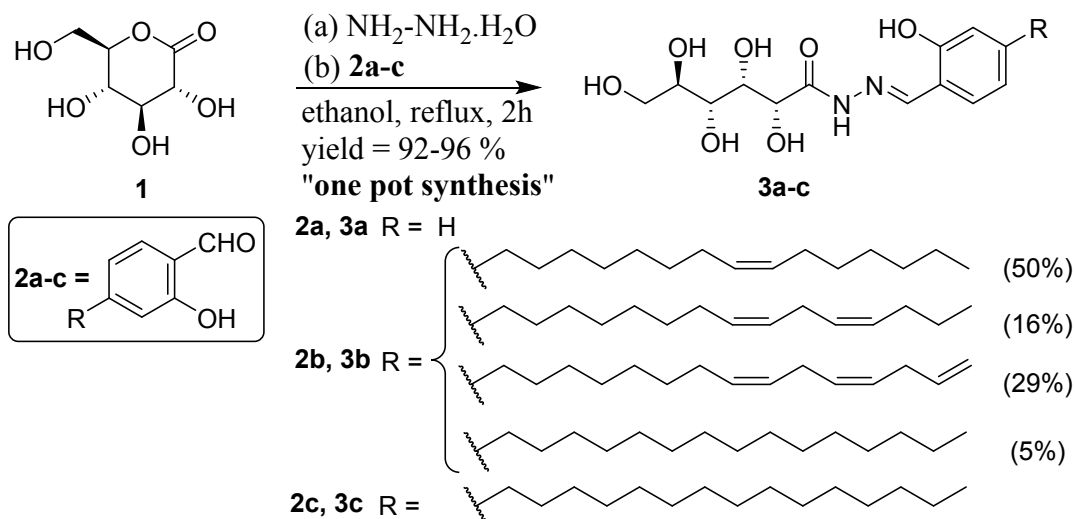


**Compound 2b** Yellow liquid; yield = 88%.  $^1\text{H}$  NMR (300 MHz,  $\text{CDCl}_3$ )  $\delta$  = 11.05 (s, 1H), 9.83 (s, 1H), 7.44 (d,  $J$  = 8.1 Hz, 1H), 6.83 (d,  $J$  = 7.8 Hz, 1H), 6.80 (s, 1H), 5.39-5.33 (m, 2H), 2.61 (t,  $J$  = 7.5 Hz, 2H), 2.05-1.93 (m, 2H), 1.64-1.59 (m, 4H), 1.37-1.24 (m, 16H), 0.88 (t,  $J$  = 6.9 Hz, 3H);  $^{13}\text{C}$  NMR (75 MHz,  $\text{CDCl}_3$ )  $\delta$  = 195.80, 161.80, 153.82, 133.58, 130.00, 129.74, 120.50, 118.85, 117.07, 36.44, 32.62, 31.80, 30.66, 29.74, 29.72, 29.67, 29.63, 29.44, 29.34, 29.25, 29.21, 29.16, 29.00, 27.24, 27.17, 22.67, 14.12.

**Compound 2c** White crystalline solid; Yield = 92%.  $^1\text{H}$  NMR (300 MHz,  $\text{CDCl}_3$ )  $\delta$  = 11.05 (s, 1H), 9.83 (s, 1H), 7.45 (d,  $J$  = 7.8 Hz, 1H), 6.83 (dd,  $J$  = 7.8, 1.5 Hz, 1H), 6.80 (s, 1H), 2.61 (t,  $J$  = 7.8 Hz, 2H), 1.66-1.57 (m, 2H), 1.34-1.24 (m, 24H), 0.88 (t,  $J$  = 6.9 Hz, 3H);  $^{13}\text{C}$  NMR (75 MHz,  $\text{CDCl}_3$ )  $\delta$  = 195.78, 161.79, 153.82, 133.57, 120.49, 118.84, 117.07, 36.45, 31.94, 30.67, 29.71, 29.67, 29.65, 29.54, 29.44, 29.38, 29.25, 22.71, 14.13.

### General Procedure for the Synthesis of Sugar Based Amphiphiles (3a-c)

To gluconolactone (1.0 mmol) in ethanol hydrazine hydrate (1.5 mmol) was added and refluxed for 30 min. After 30 min, 2-hydroxy-4-alkylbenzaldehyde (**2a-c**) (1.0 mmol) was added and further refluxed for 90 min. The progress of the reaction was monitored by performing TLC. After completion of the reaction, the reaction mixture was cooled to room temperature and the precipitated solid was filtered and dried.



### Compound 3a

Isolated as white solid;  $^1\text{H NMR}$  ( $\text{DMSO-}d_6$ , 300 MHz)  $\delta$  = 11.49 (s, 1H, Ar-OH), 11.39 (s, 1H, -NH), 8.60 (s, 1H, -CH=N), 7.43 (dd,  $J$  = 8.1, 1.8 Hz, 1H, Ar-H), 7.29 (t,  $J$  = 8.1 Hz, 1H, Ar-H), 6.90 (dd,  $J$  = 8.1, 6.0 Hz, 2H, Ar-H), 5.64 (d,  $J$  = 5.1 Hz, 1H, Sac-H), 4.62 - 4.54 (m, 3H, Sac-H), 4.39 (t,  $J$  = 5.4 Hz, 1H, Sac-H), 4.21 (t,  $J$  = 4.5 Hz, 1H, Sac-H), 4.02-3.95 (m, 1H, Sac-H), 3.62-3.58 (m, 1H, Sac-H), 3.52-3.49 (m, 2H, Sac-H);  $^{13}\text{C NMR}$  ( $\text{CDCl}_3$ , 75 MHz)  $\delta$  = 170.67, 169.00, 157.38, 148.55, 131.26, 129.78, 119.30, 118.40, 116.35, 73.37, 71.86, 71.45, 70.41, 63.23. HRMS (ESI):  $m/z$  calcd for  $\text{C}_{13}\text{H}_{18}\text{N}_2\text{O}_7$  = 314.1114; observed  $[\text{M}+\text{H}]^+$  =  $m/z$  315.4376.

### Compound 3b

Isolated as pale white solid;  $^1\text{H NMR}$  ( $\text{DMSO-}d_6$ , 300 MHz)  $\delta$  = 11.43 (s, Ar-OH), 11.38 (s, -NH), 10.16 (s, Ar-OH), 8.55 (s, -CH=N), 7.58 (d,  $J$  = 8.4 Hz, 1H, Ar-H), 7.29 (d,  $J$  = 7.8 Hz, 1H, Ar-H), 6.80-6.72 (m, 2H, Ar-H), 5.62 (d,  $J$  = 5.1 Hz, 1H, Sac-H), 5.34-5.30 (m, 2H, -CH=CH<sub>2</sub>), 4.60-4.53 (m, 3H, Sac-H), 4.37 (t,  $J$  = 5.7 Hz, 2H, Sac-H), 4.20 (t,  $J$  = 4.5 Hz, 1H, Sac-H), 3.99 (s, 1H, Sac-H), 3.58-3.40 (m, 3H, Sac-H), 2.59-2.53 (m, 2H), 2.0-1.97 (m, 4H), 1.56-1.53 (m, 4H), 1.35-1.25 (m, 14H), 0.88 - 0.83 (m, 3H);  $^{13}\text{C NMR}$  ( $\text{CDCl}_3$ , 75 MHz)  $\delta$  = 190.13, 168.94, 167.20, 159.12, 155.86, 150.51, 147.13, 144.67, 139.82, 128.11, 118.51, 118.33, 114.88, 114.39, 71.79, 70.29, 69.88, 68.79, 61.65, 33.72, 33.47, 29.46, 28.52, 27.41, 27.32, 26.99, 26.89, 26.61, 24.92, 23.55, 20.41, 19.49, 12.24. HRMS (ESI):  $m/z$  calcd for  $\text{C}_{28}\text{H}_{46}\text{N}_2\text{O}_7$  = 522.3305; observed  $[\text{M}+\text{H}]^+$  =  $m/z$  523.5875.

Note: Because of the possible E-Z isomerization of compound 3b, two different signals for proton and carbon were observed.

### Compound 3c

Isolated as white solid;  $^1\text{H}$  NMR ( $\text{DMSO-}d_6$ , 300 MHz)  $\delta$  = 11.43 (s, 1H), 11.38 (s, 1H), 8.55 (s, 1H,  $-\text{CH}=\text{N}$ ), 7.29 (d,  $J$  = 8.1 Hz 1H, Ar-H), 6.80–6.71 (m, 2H, Ar-H), 5.62 (d,  $J$  = 5.1 Hz, 1H, Sac-H), 5.48 (d,  $J$  = 5.4 Hz, 1H, Sac-H), 4.61–4.54 (m, 3H, Sac-H), 4.41–4.33 (m, 2H, Sac-H), 4.20–4.15 (m, 2H, Sac-H), 3.54–3.48 (m, 2H, Sac-H), 2.59–2.53 (m, 2H), 1.59–1.54 (m, 2H), 1.35–1.25 (m, 24H), 0.88–0.83 (m, 3H);  $^{13}\text{C}$  NMR ( $\text{CDCl}_3$ , 75 MHz)  $\delta$  = 170.68, 168.90, 157.57, 148.85, 146.40, 129.91, 119.59, 116.10, 72.97, 71.65, 71.54, 70.45, 63.46, 35.18, 31.35, 30.54, 29.07, 28.78, 22.15, 13.97. HRMS (ESI):  $m/z$  calcd for  $\text{C}_{28}\text{H}_{48}\text{N}_2\text{O}_7$  = 524.3462; observed  $[\text{M}+\text{H}]^+ = m/z$  525.6153.

Note: Because of the possible E-Z isomerization of compound 3c, two different signals for proton and carbon were observed.

### Gelation Studies

A known quantity of gelator was mixed with appropriate amount of solvent in a sealed test tube, and the system was heated to 90-120 °C until the solid was dissolved. By this procedure the solvent boiling point becomes higher than that under standard atmospheric pressure. The resulting solution was allowed to cool slowly to room temperature, and gelation was visually observed by inverting the test tube. A gel sample that exhibited no gravitational flow in inverted tube was obtained. It is denoted as “G”. Instead of forming gel if it remains as solution at the end of the tests then it is referred to as “S” (solution) and if it remain as precipitate, the system was denoted as “P” (precipitation). The system, in which the gelator is not soluble even at the boiling point of the solvent, was called an insoluble system (I).

**Table S1.** Solvents/Oils used for gelation studies

S.No	Solvents/Oils	Observation <sup>a</sup> (CGC w/v%)		
		3a	3b	3c
1	Hazelnut oil	I	S	S
2	Sesame oil	I	S	<b>G(1.0)</b>
3	Jjoba oil	I	S	S
4	Olive oil	I	<b>G(1.0)</b>	<b>G(0.5)</b>
5	Soybean oil	I	S	<b>G(0.8)</b>
6	Linseed oil	I	<b>G(1.0)</b>	<b>G(0.8)</b>
7	Light paraffin oil	I	I	I
8	Heavy paraffin oil	I	I	PG

9	Eucalyptus oil	I	S	PG
10	Neem oil	I	S	<b>G(0.5)</b>
11	Castor oil	I	P	<b>G(0.8)</b>
12	Silicone oil	I	<b>G(1.0)</b>	<b>G(0.8)</b>
13	Diesel	I	<b>G(1.0)</b>	<b>G(1.0)</b>
14	Heptane	I	I	I
15	Dioxane	I	I	I
16	THF	I	I	I
17	Dodecanol	P	P	<b>G(1.0)</b>
18	Octanol	P	I	P
19	Ethanol	I	I	I
20	Butanol	P	I	I
21	Isopropanol	I	I	I
22	Toluene	I	I	I
23	Benzene	P	I	I
24	<b>1,2-Dichlorobenzene</b>	S	<b>G(1.0)</b>	<b>G(0.5)</b>
25	Xylene	P	P	P
26	DMF	S	S	S
27	DMSO	S	S	S
28	WATER	S	P	I
29	Acidic Buffer	I	I	I
30	Basic Buffer	I	I	I
31	DMSO+Water	P	P	P

<sup>a</sup>S = soluble; I = Insoluble; P = Precipitate; G = Gel; PG = Partial Gel

### Morphological Analysis

Morphology of the gel was studied using Carl Zeiss AXIO ScopeA1 fluorescent/phase contrast microscope. A glass slide containing a small portion of gel was mounted on Phase Contrast Microscope and the morphology of gel was identified. Morphology of self-assembled structure formed by **3c** and its corresponding Cu<sup>2+</sup> induced morphological transition was studied using JEOL JEM 2100 F FETEM.

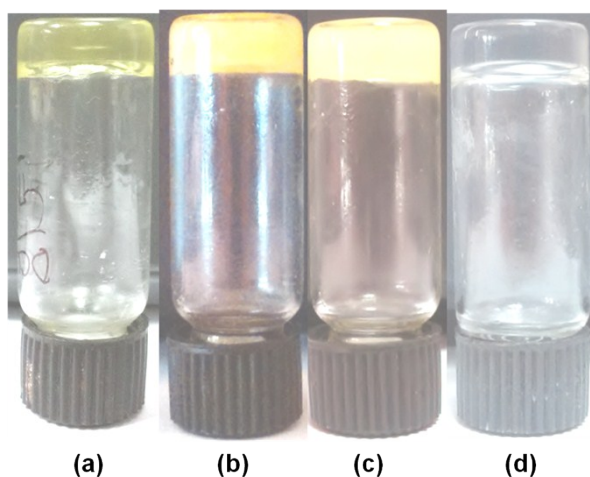


**Figure S1.** (a-d) Photographs of gel formed by (a) **3b** in 1,2-DCB; (b) **3b** in olive oil; (c) **3c** in olive oil and (d) **3c** in 1,2-DCB.

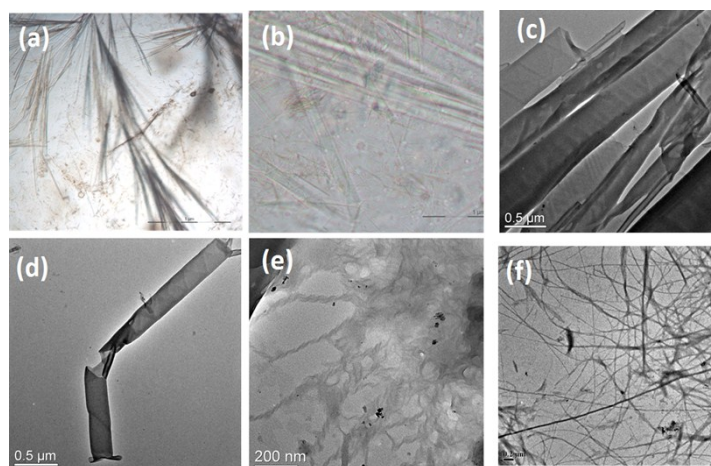


**Figure S2.** Optical micrographs of (a) **3b** 1,2-DCB and (b) **3c** in 1,2-DCB. HRTEM images of (c & d) **3c** in 1,2-DCB, (e) **3b** in water and (f) **3c** in water.

### ATR-FTIR Studies

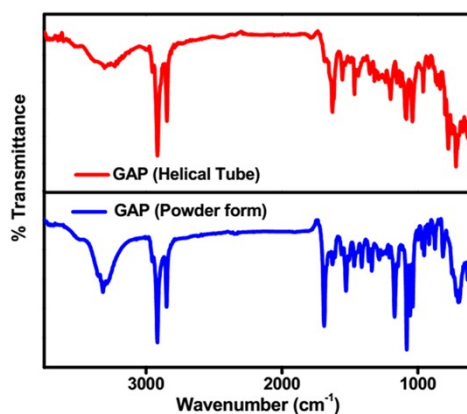


**Figure S3.** ATR-FTIR spectra of GAP in powder form and helical tubular form.

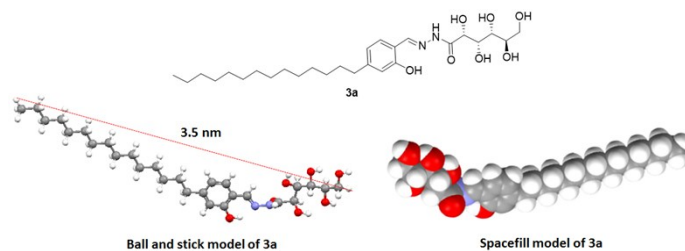


**Figure S4.** Energy minimized structure of GAP.

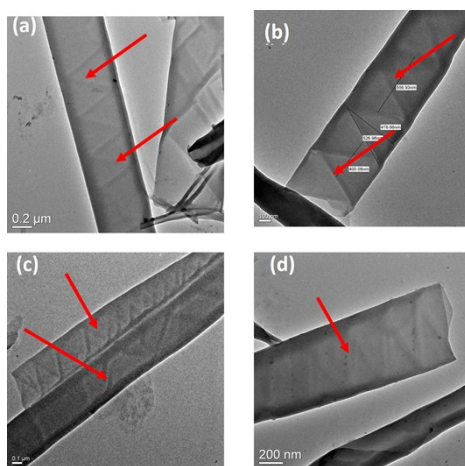


**Figure S5.** HRTEM images of individual helical tubules in gel formed by GAP in 1,2-DCB displaying helical marking.

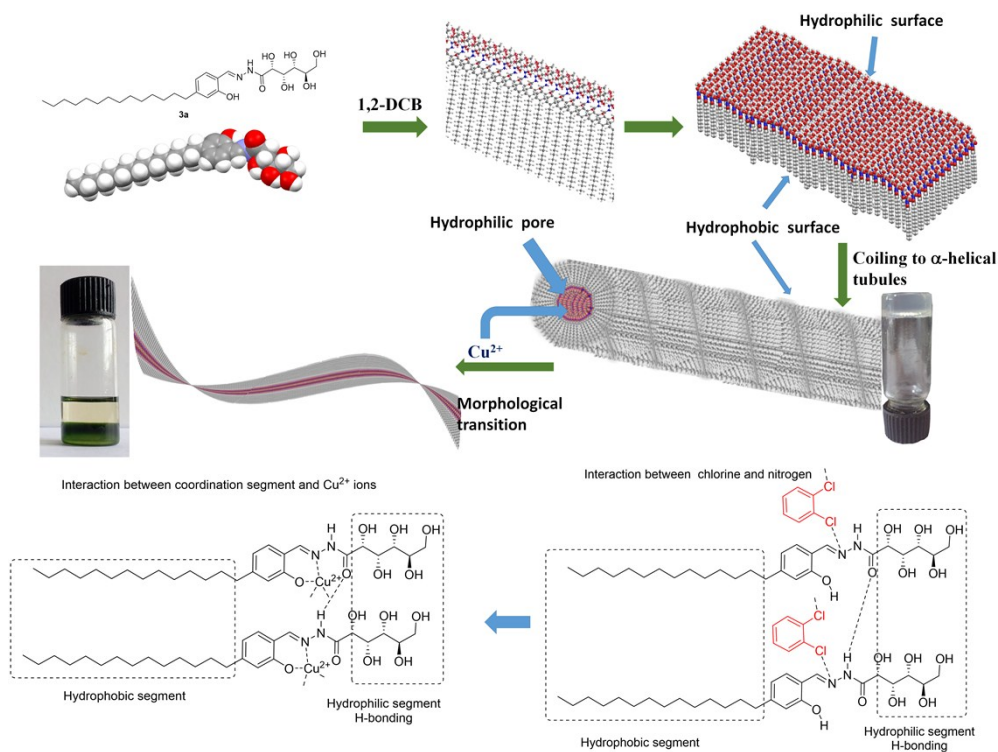


**Figure S6.** Mechanism for the formation of individual helical tubules in gel formed by GAP in 1,2-DCB displaying helical marking.



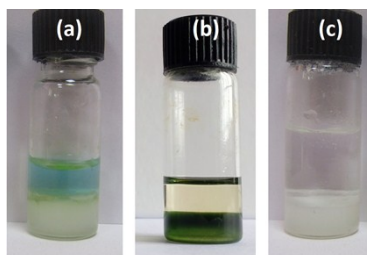


**Figure S7** . Response of gel formed by GAP in 1,2-DCB after the addition of  $\text{Cu}(\text{OAc})_2$  dissolved in water (a),  $\text{Cu}(\text{OAc})_2$  dissolved in ethanol:1,2-DCB (1:9 ratio) (b) and double distilled water (c).

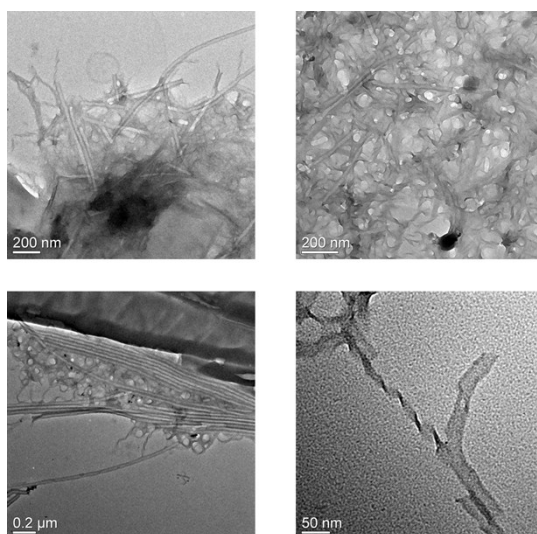


**Figure S8**. HRTEM images of  $\text{Cu}^{2+}$  induced randomly twisted fibers from helical tubules.

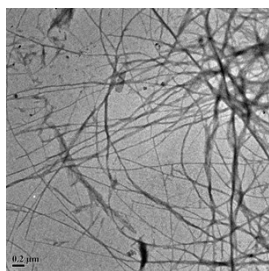


**Figure S9**. HRTEM image of fiber formation of GAP in water.

### UV/ Visible and Circular Dichroism (CD) Spectroscopy

UV/vis spectra were recorded on Thermo Scientific Evolution 220 UV/visible spectrophotometer. The spectra were recorded in the continuous mode between 200 and 700 nm, with a wavelength increment of 1 nm and a bandwidth of 1 nm.

CD spectra were obtained using JASCO J-815 CD spectrometer. The instrument was operated at a nitrogen atmosphere level of 5 LPM in the standard sensitivity range. The samples were loaded in a quartz cuvette of 0.1 cm path length

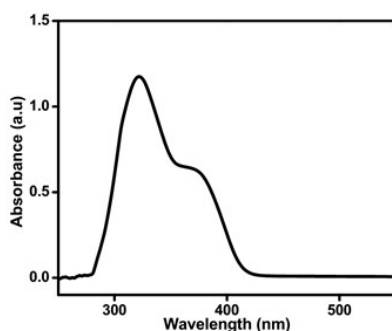


**Figure S10.** UV absorption spectra of gelator **3c** in 1,2-DCB..

### X-ray Photoelectron Spectroscopy (XPS)

XPS spectra of helical tubules and randomly twisted fiber formation triggered by  $\text{Cu}^{2+}$  were recorded on Thermofisher scientific, UK, K-Alpha surface analysis model using Al-X-ray in a wide range of 0-1350 eV.

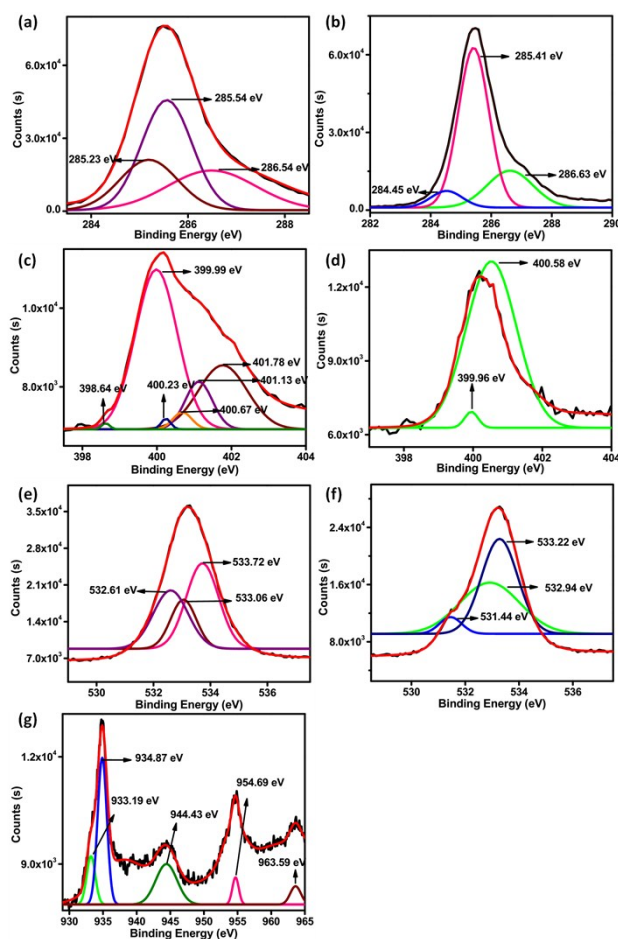


**Figure S11.** (a-g) XPS spectra of helical tubules and randomly twisted fiber formation triggered by  $\text{Cu}^{2+}$  fitted using Gaussian-Lorentzian peak: (a) C 1s, (c) N 1s and (e) O 1s spectra of helical tubules; (b) C 1s, (d) N 1s, (f) O 1s and (g) Cu 2p spectra of randomly twisted fiber formation triggered by  $\text{Cu}^{2+}$ .

## Emission studies

Emission spectra were measured on a JASCO spectrofluorometer FP-8200, by fixing the excitation value at 310 nm for 1,2-DCB solvent. Samples for absorption and emission measurements were contained in 1 cm X 1 cm quartz cuvette

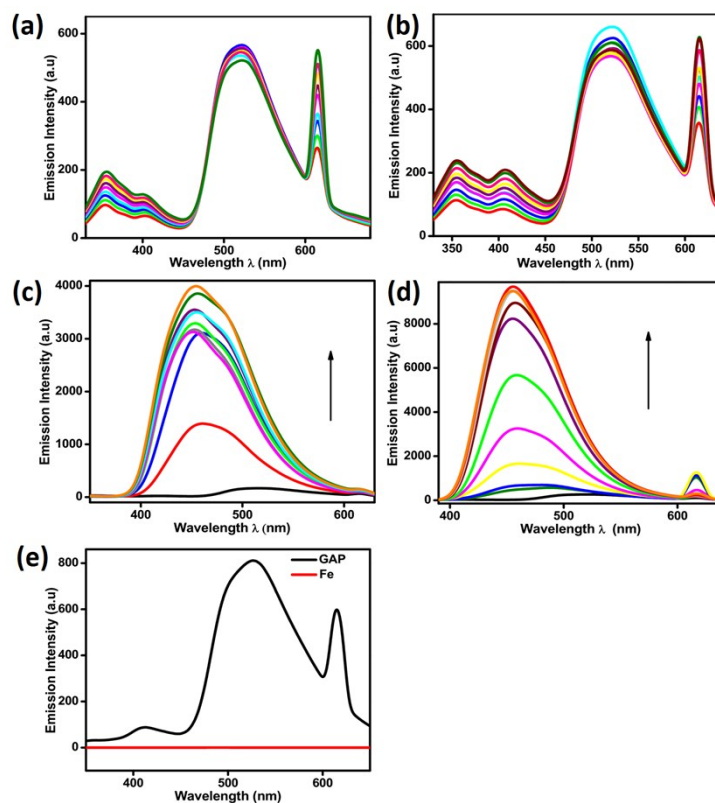


**Figure S12.** (a-e) Emission spectra of helical tubules in 1,2-DCB and its response to metal ions (a) Ca<sup>2+</sup>; (b) Mg<sup>2+</sup>; (c) Zn<sup>2+</sup>; (d) Al<sup>3+</sup>; (e) Fe<sup>3+</sup>. In titration experiments, direction of arrow shows the response of emission intensity with piecemeal addition of 100  $\mu$ L of corresponding M<sup>n+</sup> solution. 2 mL of initial volume of solution ( $1 \times 10^{-5}$ M) was taken for titration experiments.

## Phase transition of gel in response to metal ions

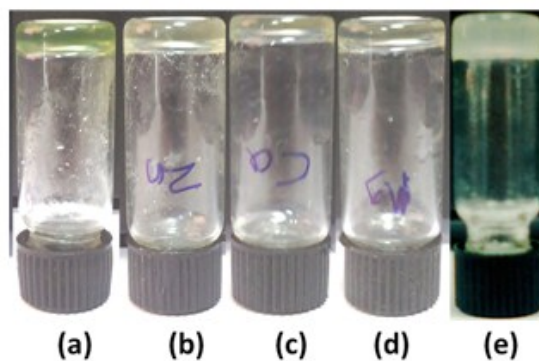


**Figure S13 .** Phase transition of gel formed by **GAP** in DCB in response to (a) Cu<sup>2+</sup>; (b) Zn<sup>2+</sup>; (c) Ca<sup>2+</sup> (d) Mg<sup>2+</sup> and (e) Al<sup>3+</sup>.

## Morphological transition of gel in response to metal ions

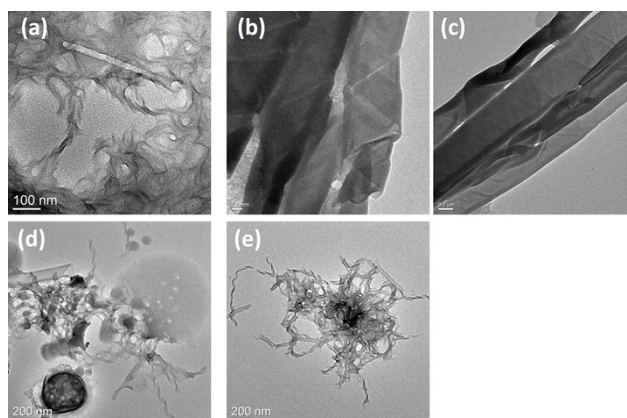


**Figure S14** . HRTEM images of **GAP** in 1,2-DCB in response to (a)  $\text{Cu}^{2+}$ ; (b)  $\text{Zn}^{2+}$ ; (c)  $\text{Ca}^{2+}$  (d)  $\text{Mg}^{2+}$  and (e)  $\text{Al}^{3+}$ .

### 1. Rheological Measurements

The mechanical properties of gel were investigated with a stress controlled rheometer (Anton Paar 302 rheometer) equipped with a steel-coated parallel-plate geometry (25 mm diameter). The gap between two plates was 1 mm. The measurements were carried out at 23 °C. The amplitude sweep measurement was conducted first. This provides the information about linear viscoelastic range which is directly proportional to the mechanical strength of the gel sample. This frequency sweep was then performed to monitor the storage modulus,  $G'$  and the loss modulus,  $G''$  as functions of frequency sweep from 0.1 to 300  $\text{rad s}^{-1}$ .

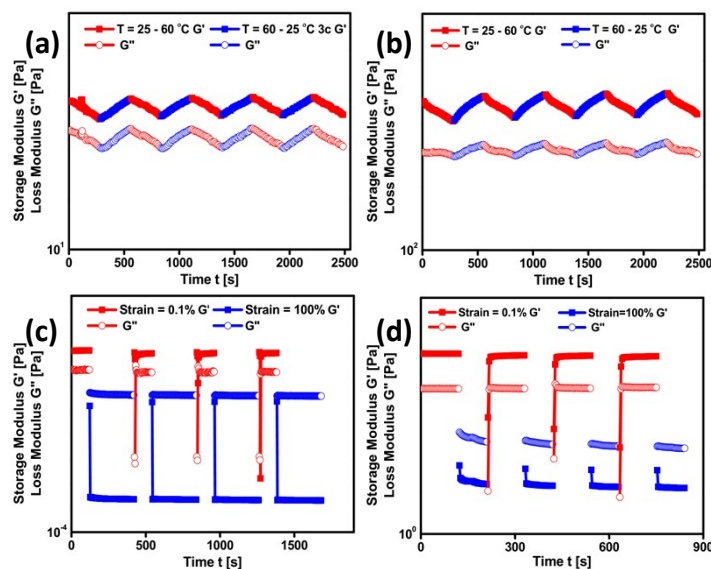


**Figure S15**. (a - d) Time course change of storage ( $G'$ ) and loss ( $G''$ ) modulus in (a and b) temperature ramp experiment and (c and d) step strain experiment of gel formed by GAP in 1,2-DCB (a,c) after the addition of  $\text{Cu}^{2+}$  solution on gel formed by GAP in 1,2-DCB (b,d) respectively

**Table S2.** Metal ion induced phase and morphological transition of gel formed by GAP in 1,2-DCB.

Metal ion	Emission intensity	phase transition	Morphological transition	Morphology
Cu <sup>2+</sup>	Decrease	No (gel)	Yes	Twisted fibers
Ca <sup>2+</sup>	No effect	No (gel)	No	Helical tubules
Mg <sup>2+</sup>	No effect	No (gel)	No	Helical tubules
Zn <sup>2+</sup>	Increase	No (gel)	Yes	Twisted fibers
Al <sup>3+</sup>	Increase	No (gel)	Yes	Twisted fibers
Fe <sup>3+</sup>	Decrease	Yes (sol)	Yes	-

## 2. NMR and Mass Measurements

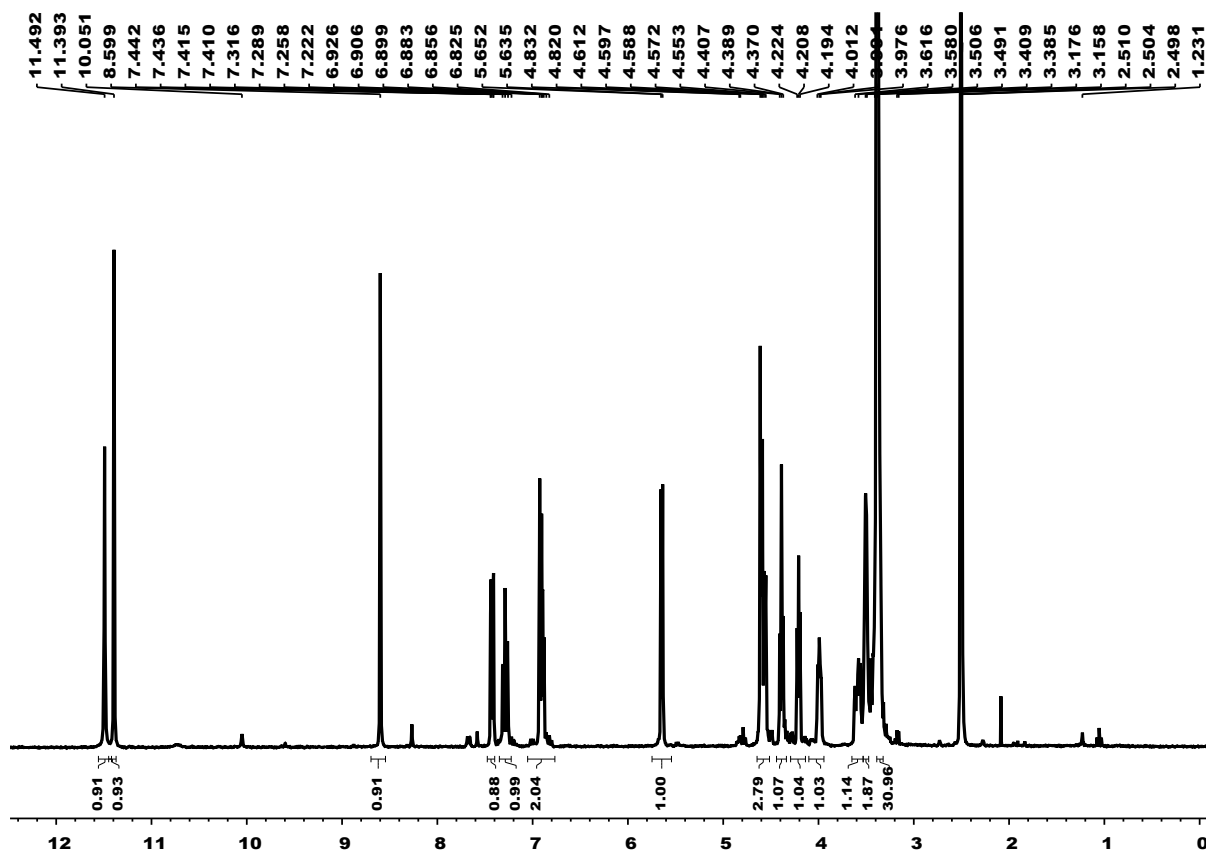


Figure S16.  $^1\text{H}$  NMR of compound, **3a** in  $\text{DMSO-}d_6$  at 300 K

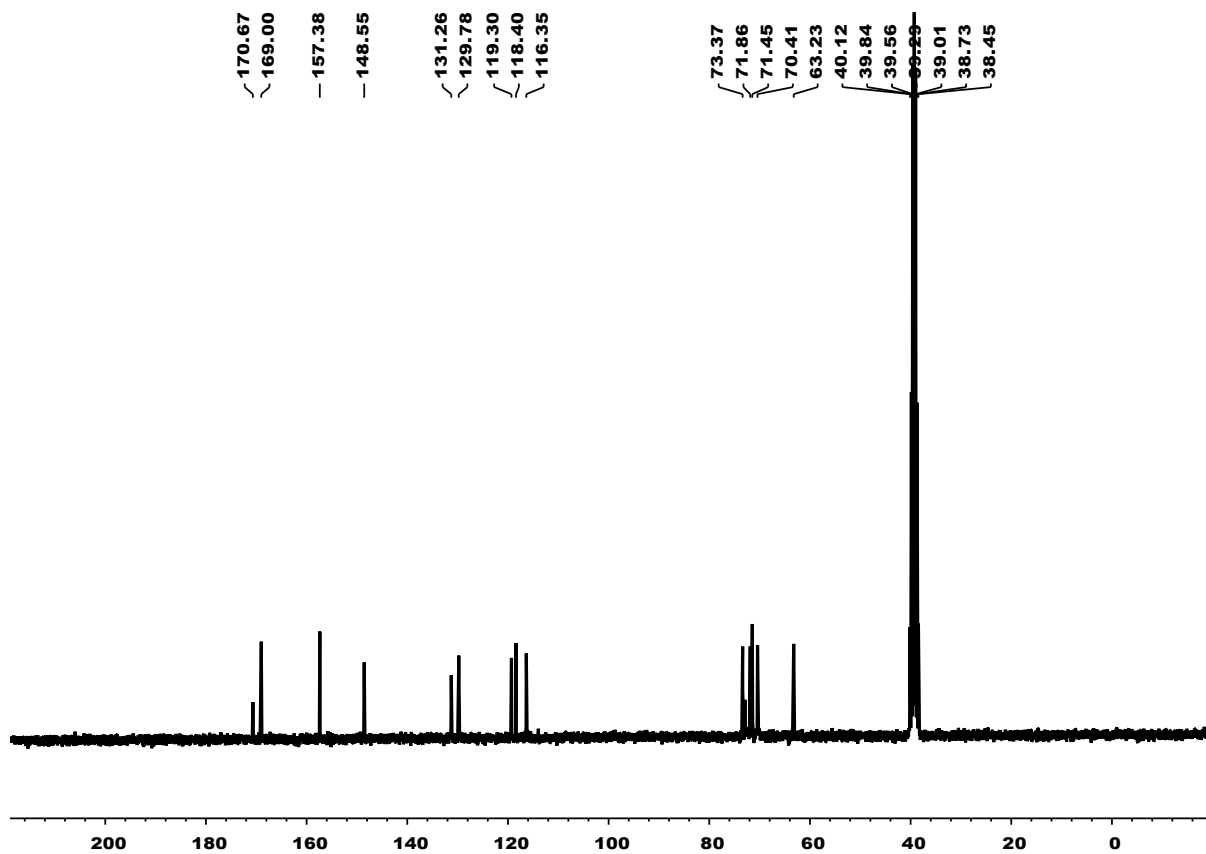


Figure S17.  $^{13}\text{C}$  NMR of compound, **3a** in  $\text{DMSO-}d_6$  at 300 K

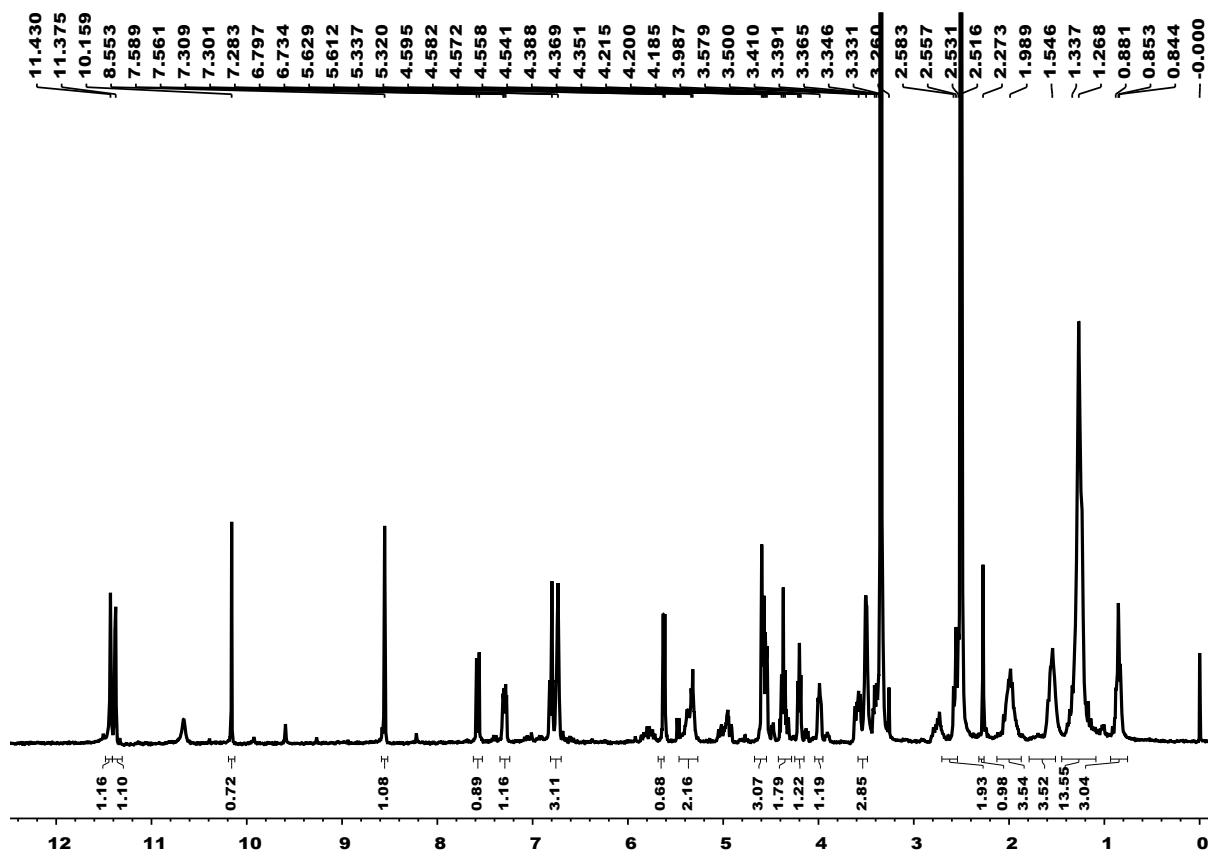


Figure S18.  $^1\text{H}$  NMR of compound, **3b** in  $\text{DMSO-}d_6$  at 300 K

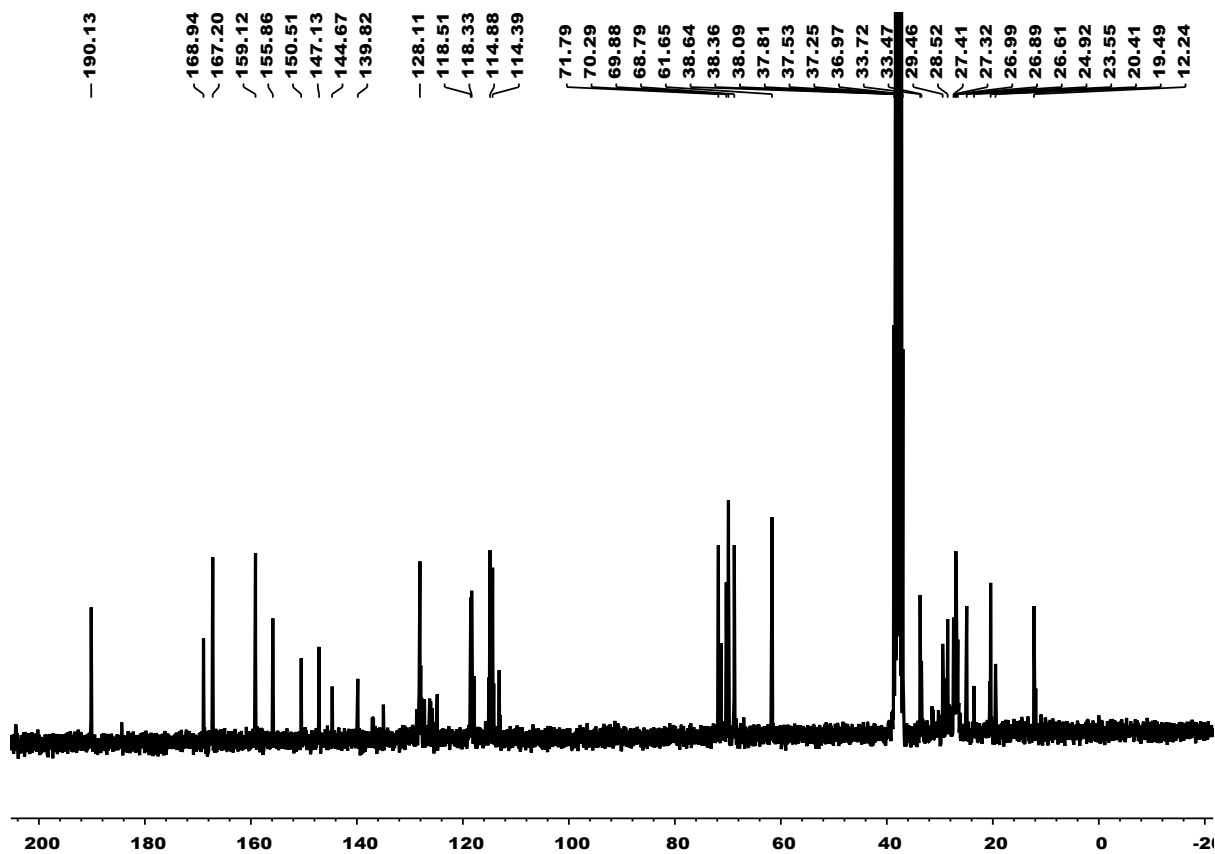


Figure S19.  $^{13}\text{C}$  NMR of compound, **3b** in  $\text{DMSO-}d_6$  at 300 K

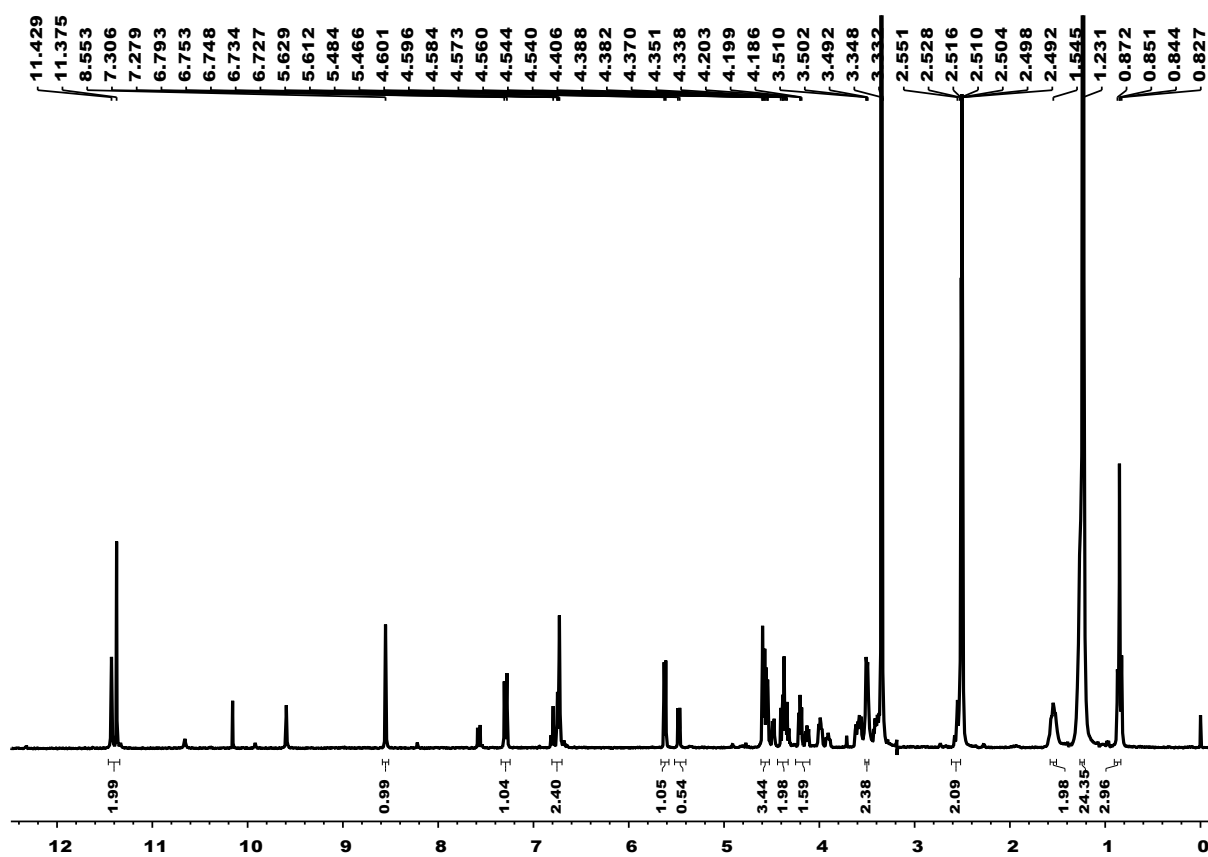


Figure S20.  $^1\text{H}$  NMR of compound, **3c** in  $\text{DMSO-}d_6$  at 300 K

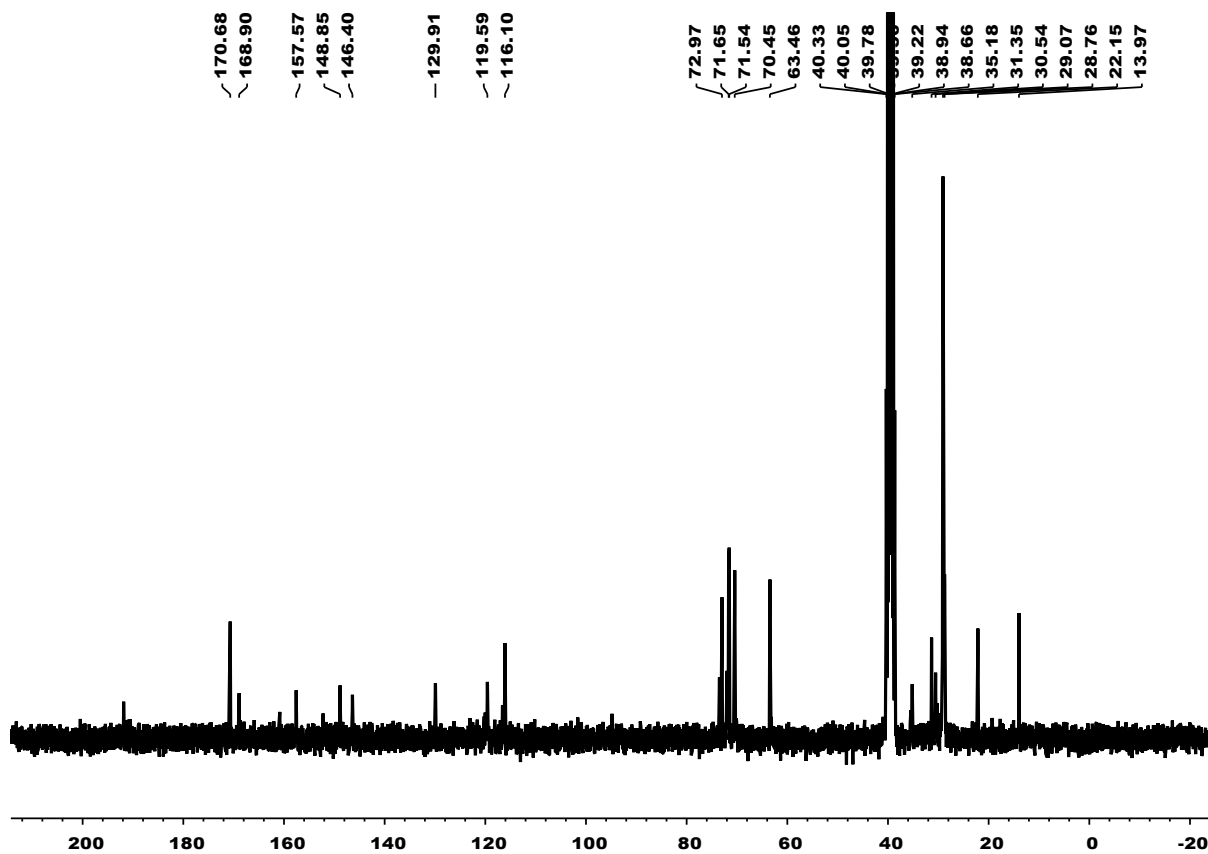


Figure S21.  $^{13}\text{C}$  NMR of compound, **3c** in  $\text{DMSO-}d_6$  at 300 K



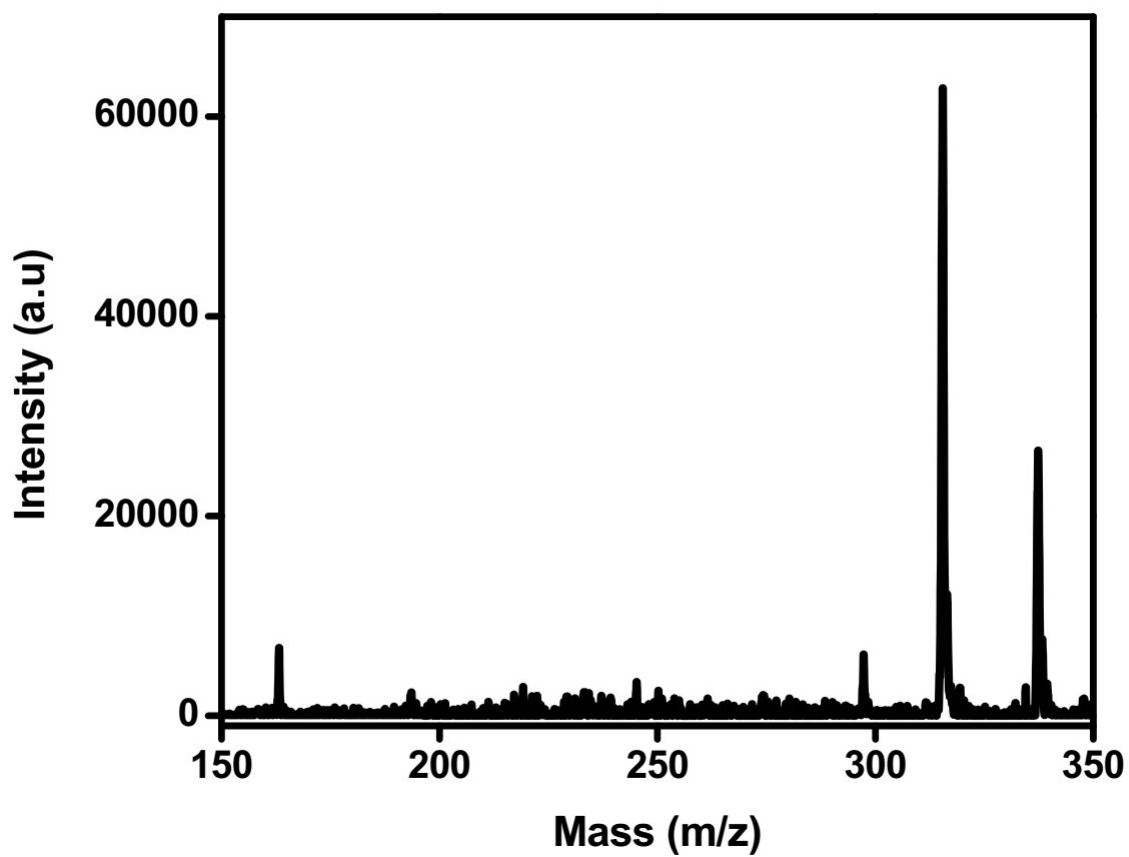


Figure S22. Mass spectra of 3a

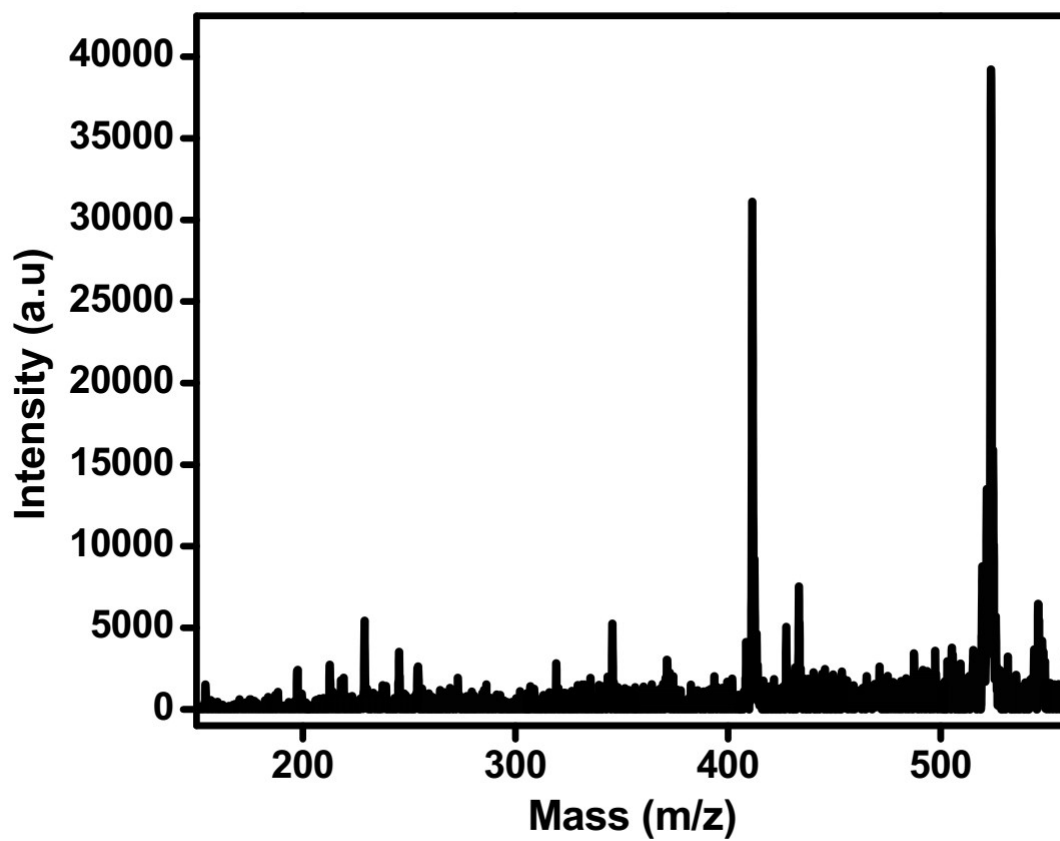


Figure S23. Mass spectra of 3b

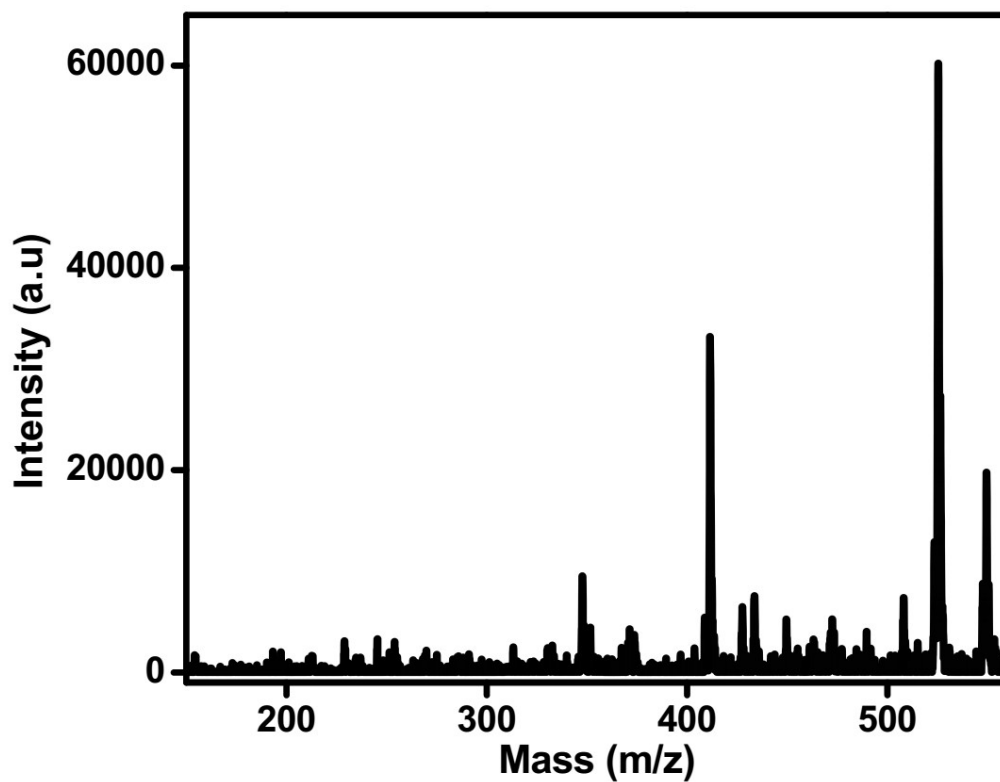


Figure S24. Mass spectra of 3c

---

(a) Lalitha, K.; Jenifer, P.; Prasad, Y. S.; Muthusamy, K.; John, G.; Nagarajan, S. *RSC Adv.* 2014, 4, 48433-48437; (b) Lalitha, K.; Nagarajan, S.. *J. Mater. Chem. B.* 2015, 3, 5690-5701;